Article

Not peer-reviewed version

Water Flow in the Soil Profile Under an Agroforestry System in the Colombian Amazon Based on HYDRUS-1D Model

Fabio Buriticá , Juan Carlos Suárez * , Fausto Andres Ortiz-Morea

Posted Date: 20 October 2023

doi: 10.20944/preprints202310.1283.v1

Keywords: soil hydraulic properties; spatial variation; soil water simulation; soil water flow

Article

Water Flow in the Soil Profile under an Agroforestry System in the Colombian Amazon Based on HYDRUS-1D Model

Fabio Buriticá [1,2], Juan Carlos Suárez [3,4,*] and Fausto Andrés Ortiz-Morea [3,4]

1 Programa de Doctorado en Ciencias Naturales y Desarrollo Sustentable, Facultad de Ciencias Agropecuarias, Universidad de la Amazonia, 180002 Florencia, Colombia. f.buritica@udla.edu.co (F.B.)
2 Programa de Matemáticas y Física, Facultad de Educación, Universidad de la Amazonia, 180002 Florencia, Colombia
3 Programa de Ingeniería Agroecológica, Facultad de Ingeniería, Universidad de la Amazonia, 180002 Florencia, Colombia. ju.suarez@udla.edu.co (J.C.S.), fua.ortiz@udla.edu.co (F.A.O-M.)
4 Centro de Investigaciones Amazónicas CIMAZ Macagual Cesar Augusto Estrada González, Grupo de Investigaciones Agroecosistemas y Conservación en Bosques Amazónicos- GAIA
* Correspondence: ju.suarez@udla.edu.co; Tel.: +57 3202804455

Abstract: Knowledge of water availability in terms of spatial (i.e., depth) and temporal variability of soil water is essential to describe soil water infiltration and storage processes accurately. Therefore, performing simulations of soil water dynamics can be a valuable tool to evaluate different land uses and their impact on water availability. Consequently, this study aimed to model the volumetric soil water content (θ, cm^3 cm^{-3}) under agroforestry systems (AFS) with cocoa. For this purpose, the θ was monitored at different depths (0-20, 20-40, 40-60, 60-80, 80-100 cm) in the soil profile of four plots (20 × 50 m) of cocoa under agroforestry systems. Environmental conditions significantly influenced the water balance of the cocoa crop. There were seven moments when evapotranspiration (ET_0) was higher than 5 mm d^{-1}. During those moments, the environment exhibited higher PAR values of 1041 μmol m^{-2} s^{-1}, very low atmospheric relative humidity (RH_a) levels (around 45%), higher ambient temperatures of 32.2 ºC and a vapor pressure deficit of 1.6 kPa whose θ levels reached 0.32 cm^3 cm^{-3} and a water balance of -5.7 mm, which presented negative values during most of the study period. The θ obtained from the HYDRUS-1D model presented a slight bias as a high level of coherence between the observed values, based on the model's goodness-of-fit estimators. The above provides accurate simulations of soil water content at various depths, much-needed information for management schemes for cocoa cultivation under agroforestry systems.

Keywords: Soil hydraulic properties; Spatial variation; Soil water simulation; Soil water flow; Richards equation

1. Introduction

Soil water availability is an essential variable for hydrological understanding[1], which is influenced by factors such as environmental conditions (precipitation, evapotranspiration, radiation [2]), soil physical properties[3,4], crop management[5,6], composition and structure under agroforestry arrangements [7–10]. In this sense, the importance of soil water monitoring has been reported by different studies[11–13], among which the generation of management and adaptation schemes[2] in crops such as cocoa[7,14] stands out.

Regarding soil hydraulics, soil structure controls retention functions and hydraulic conductivity[15]. In this sense, knowing the spatial (i.e., at depth level) and temporal variability of water in the soil is fundamental to accurately describing the processes of infiltration and water storage[16]. Therefore, performing simulations of soil water dynamics can be a valuable tool to evaluate different land uses and their impact on water availability [17].

Developing accurate simulations requires that the hydraulic properties of the soil, i.e., hydraulic conductivity and water retention, are adequately known. These parameters can be derived from soil physical properties using pedotransfer functions from direct or inverse measurements[18], or through models[19,20], whose objective is the assessment of water availability in the soil profile to determine states of water deficit [21–23] that affect crops development.

Cocoa is grown under different agroforestry structures[24], which impacts the water status of cocoa trees[25,26]; therefore, knowing the dynamics of soil drainage under cocoa production systems is important for managing a proper water balance. Understanding the dynamics of soil drainage is necessary to know the water demand because when there are situations of stress caused by water deficit, physiological processes such as photosynthesis are affected[27–30], resulting in adverse effects on production[14,31,32]. According to the above and based on characteristics such as water availability in the soil profile, physical properties, hydraulic properties and precipitation, the objective of this study was to model the volumetric soil water content (θ, cm^3 cm^{-3}) under agroforestry systems (AFS) with cocoa (*Theobroma cacao*) as the main crop in the Colombian Amazon. The information generated will give a better understanding of the dynamics of soil drainage in agroforestry systems in the Amazon under drought conditions, which may become more frequent and severe due to climate change[7,33].

2. Materials and Methods

2.1. Study site and monitoring of environmental variables under agroforestry systems

The study was conducted in a cocoa agroforestry arrangement at the Macagual Research Center - University of Amazonia-Colombia (1°37′N y 75°36′W). This region presents a warm-humid climate, characteristic of the tropical rainforest ecosystem, with an average annual rainfall of 3,800 mm, a sunshine of 1,700 hours $year^{-1}$, an average temperature of 25.5°C and relative air humidity of 84%. Four cocoa plots (20 × 50 m) were established into a cocoa agroforestry system. The agroforestry system is composed of cocoa plants planted at a distance of 3 × 3 m and timber species such as *Cariniana pyriformis* and *Calycophyllum spruceanum* with a density of 55 trees per ha^{-1} that generate a transmitted radiation of 28%, exhibiting a typology classified as diversified multistrata shade[24].

Monitoring was carried out in each plot, from day of year 66 to 85 of 2015 (March 7 to 25). A WatchDog 2900ET (Spectrum Technologies, Inc., USA) meteorological station was placed under the canopy of the agroforestry arrangement at the height of 1.5 m, and the precipitation (PP mm), air relative humidity (RH_a %), air temperature (Ta, ºC), and photosynthetically active radiation (PAR, µmol m^{-2} s^{-1}) monitored every minute. The vapor pressure deficit (VPD, kPa) was calculated from the air temperature and relative humidity recorded minute by minute following the methodology proposed by Allen et al.[34]. With the different environmental variables, the reference daily evapotranspiration (ET_0; mm day^{-1}) was calculated according to the FAO Penman-Monteith method[34]:

$$ET_0 = \frac{0.408\Delta(R_n - G) + \gamma\left({}^{900}/_{T} + 272\right)u_2(e_s - e_a)}{\Delta + \gamma(1 + 0.34u_2)} \quad (1)$$

where R_n is the net radiation absorbed by the surface [MJ m^{-2} day^{-1}], G is the ground heat flux density [MJ m^{-2} day^{-1}], T is the air temperature [◦C], u_2 is the wind speed [m s^{-1}], e_s is the saturation vapor pressure [kPa], e_a is the actual vapor pressure [kPa], Δ is the slope of the vapor pressure curve [kPa ◦ C^{-1}], γ is the psychrometric constant [kPa ◦ C^{-1}]. The climatic water balance (CWB) was calculated as PP-ET_0 according to FAO[35].

2.2. Determination of soil hydraulic characteristics and properties

The 5TE sensor (Decagon Devices Inc., Pullman, WA, USA) connected to an Em50 data logger (Decagon Devices Inc, Pullman, WA, USA) between 10 and 100 cm depth was used to monitor minute by minute the volumetric soil water content (θ, cm^3 cm^{-3}) during the monitoring period in each plot. From the texture and bulk density at each depth evaluated and using the pedotransfer function of the ROSETTA software[20], initial appreciations were derived to estimate soil hydraulic parameters (θ_s, θ_r, α ,n and K_s Table 1). This function predicts the saturated hydraulic conductivity (K_s) and the saturation point (K_0) on the saturation curve, which may differ from the K_s match. The K_0 was used as the initial parameter value of K_s (Table 1).

2.3. Modelo Hydrus-1D

To simulate water movement in the soil profile under the agroforestry system, the program Hydrus-1D[36] was used. This program numerically solves the Richards equation for water flow[36], described as follows:

$$\frac{\partial\theta}{\partial t} = \frac{\partial}{\partial Z}\left[k\left(\frac{\partial h}{\partial z} + 1\right)\right] - S(Z,t) \quad (2)$$

Where: θ is the volumetric soil water content (cm^3 cm^{-3}), t is the time (d), z is the vertical coordinate space (cm), h is the pressure height (cm), K is the hydraulic conductivity (cm d^{-1}), and S is the water uptake term by plant roots (cm^3 cm^{-3} d-

[1]). The hydraulic properties of the unsaturated soil were described using the van Genuchtene Mualem functional relationships[37] obtained from the ROSETTA software[20], as follows:

$$\theta(h) = \theta r + \frac{\theta s + \theta r}{[1 + (\alpha h)^n]^m} \quad h < 0 \tag{3}$$

$$\theta(h) = \theta s \quad h \geq 0 \tag{4}$$

$$k(h) = K_s S_e^l \left[1 + \left(1 - S_e^{l/m}\right)^m\right]^2 \tag{5}$$

$$\text{with } m = 1 - \frac{1}{n} \ y \qquad S_e = \frac{\theta - \theta r}{\theta s - \theta r} \tag{6}$$

Where: θ_s is the saturated water content (cm^3 cm^{-3}); θ_r is the residual water content (cm^3 cm^{-3}); m, α and n are empirical form factors in the water retention function, where m = 1 - 1 / n; K_s is the saturated hydraulic conductivity (cm day^{-1}); l is the form factor in the hydraulic conductivity function and Se is the relative saturation.

2.4. Data analysis

A descriptive analysis (means and frequencies of the variables) was carried out for the climatic variables (relative humidity, temperature, precipitation, vapor pressure deficit). Volumetric soil water content (θ, cm^3 cm^{-3}) values obtained through simulations with HYDRUS-1D were compared with the observations made in the Theobroma cacao agroforestry arrangement, and thus the model fit was determined[38]. The assumptions of normality and homogeneity of variance were evaluated using the residuals studied. The Bayesian and Akaike information criteria (BIC and AIC) and the adjusted R^2 were used for model selection. For model goodness-of-fit, root-mean-square error (RMSE) and Percent Bias (PBias) were calculated, as well as modeling efficiency (EF), also known as Nash-Sutcliffe Efficiency (NSE)[25]. A standard regression was used to describe the relative relationship between the observations and the simulation (slope), which allows for identifying any lag or deviation between the simulated and observed values[39]. For this purpose, scatter plots were created showing the line of fit and the line of best fit (i.e., y=x). The model's goodness of fit was evaluated using the ggof function[40] of the HydroGOF package of R-Project version 4.1.1.[41] using the implemented interface of the R platform in InfoStat[42].

3. Results

3.1. Micrometeorological conditions and soil water content under agroforestry systems

During the study period, micrometeorological conditions were monitored simultaneously (Figure 1). The radiation levels ranged from 2 to 1,242 μmol m^{-2} s^{-1} the day with an average of 380±22 μmol m^{-2} s^{-1} which influenced humidity and ambient temperature. The RH_a presented minimum values of 48.1 with an average of 80.3 during the day and minimum values of 80.5 with an average of 97.2 during the night. The temperature ranged from 21.5 to 33.5 ºC, averaging 25.5±0.1 ºC). These two variables influenced the vapor pressure deficit, which ranged from values very close to zero to 2.1 kPa with averages of 0.37±0.02 kPa. Likewise, a total of 315.7 mm of water accumulated as a result of 46 rainfall events with an average rainfall of 6.86±1.75 mm in 45.9±7.81 minutes with an intensity of 0.12±0.03 mm $minute^{-1}$. There were seven moments in which ET_0 was higher than 5 mm d^{-1}, which coincided when the environment had higher PAR values of 1041 μmol m^{-2} s^{-1}, very low atmospheric RH_a levels (around 45%), higher ambient temperatures of 32.2 ºC and a vapor pressure deficit of 1.6 kPa. During those moments, the soil volumetric water content levels reached values of 0.32 cm^3 cm^{-3} and a CWB of -5.7 mm. CWB exhibited negative values during most of the study period. The θ in the soil profile ranged from 0.32 to 0.13 cm^3 cm^{-3}, going from 0.33 cm^3 cm^{-3} at 0-20 cm depth to 0.11 m^3 m^{-3} at 80-100 cm depth, enlightened by a linear model with a high level of fit (cm^3 cm^{-3} =0.387-0.005*depth (cm), P<0.0001 r^2=0.86, Figure 2). The predicted values of θ in the soil profile obtained from the HYDRUS-1D model closely resembled the observed data (Figure 2).

Preprints (www.preprints.org) | NOT PEER-REVIEWED | Posted: 20 October 2023 doi:10.20944/preprints202310.1283.v1

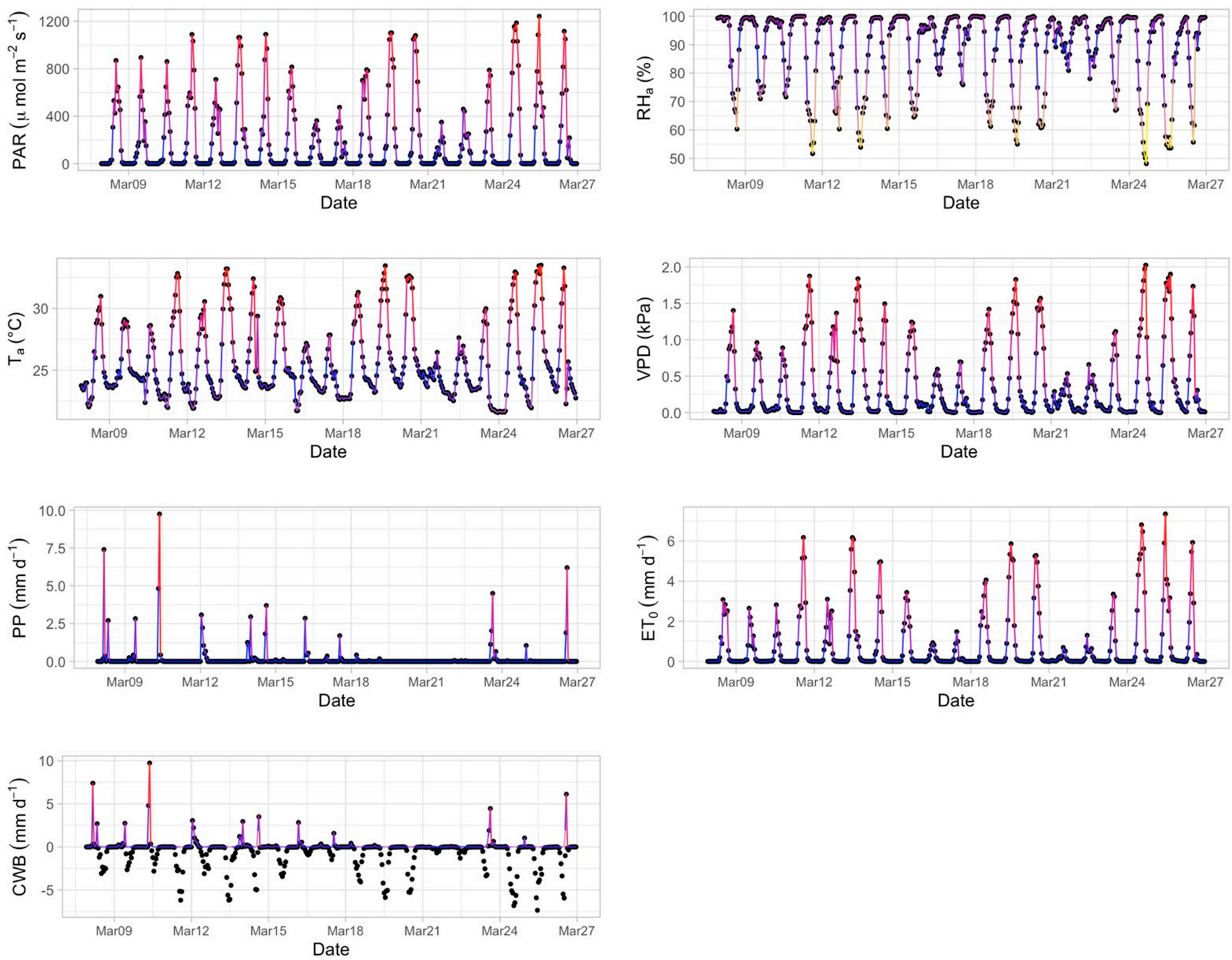

Figure 1. Diurnal patterns of photosynthetically active radiation (PAR), air relative humidity (RH_a); air temperature (T_a); vapor pressure deficit (VPD), precipitation (PP), evapotranspiration (ET_0) and climatic water balance (CWB) under a cocoa agroforestry system during the period of study. The color gradient from red, blue to yellow of the line means from higher to lower value of each variable during the diurnal pattern.

Preprints (www.preprints.org) | NOT PEER-REVIEWED | Posted: 20 October 2023 doi:10.20944/preprints202310.1283.v1

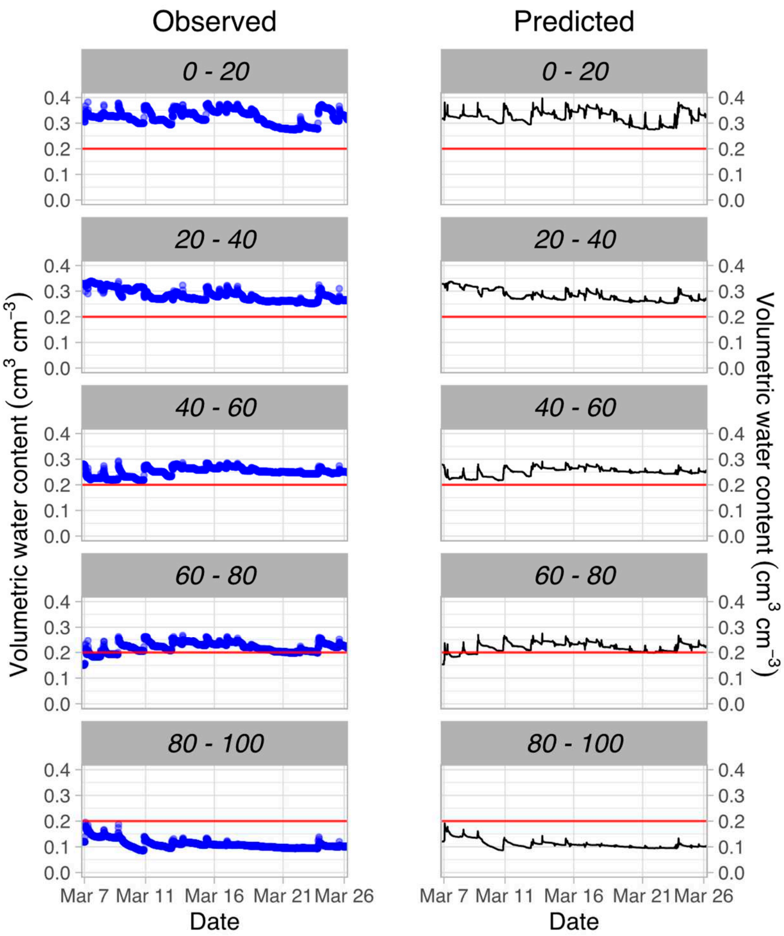

Figure 2. Diurnal pattern of volumetric water content in the soil profile under a cocoa agroforestry system: a) observed volumetric water content, and b) predicted volumetric water content.

3.2. Soil water properties

Significant differences were found for θ_f (P<0.0001), θ_r (P<0.02), θ_s (P<0.03), α (P<0.0001), n (P<0.0001), K_s (P<0.01), and K_0 (P<0.0018 at different depths (Table 1). Likewise, there were variations in relation to the level of compaction in the soil profile that affected water availability, finding a negative relationship with θ_s (r: -0.67 P<0.0001) contrary to the tendency between K_0 (r: 0.94 P<0.0001).

3.3. Hydrus-1D Calibration and Validation Model

The simulated data allowed explaining θ in each of the soil profiles, calculating each of the peaks that occur at the time of rainfall events, as well as the amount of θ as the depth increases (Figure 2). The relationship between observed versus predicted θ was estimated and simulated using the HYDRUS-1D model for each depth of the soil profile evaluated and the estimated values were found to be very close to the y=x line (Figure 3). Based on the goodness-of-fit estimators of the model, a small bias or deviation was found between the simulated and observed values measured from the RMSE, PBias and NSE, which were calculated at each depth of the soil profile (Figure 3). Likewise, a high coherence level was found, measured by R^2, which was greater than 0.96 (Figure 3).

Table 1. Soil hydraulic properties under the cocoa agroforestry system used in the HYDRUS 1D model.

Depth (cm)	ρb (g cm^{-3})		θ_f (cm^3 cm^{-3})		Equation of water retention parameters (van Genuchten Model)											
					θ_r (cm^3 cm^{-3})		θ_s (cm^3 cm^{-3})		α(cm)		n		k_s (cm d^{-1})		k_0 (cm d^{-1})	
	Mean	**S.E.**	**Mean**	**S.E.**	**Mean**	**S.E.**	**Mean**	**S.E.**	**Mean**	**S.E.**	**Mean**	**S.E.**	**Mean**	**S.E.**	**Mean**	**S.E.**
0-20	1.37	± 0.02 ^{cd}	0.286	± 0.014 ^{ab}	0.074	± 0.004 ^{a}	0.438	± 0.007 ^{a}	1.83	± 0.05 ^{ab}	1.6	± 0.04 ^{bc}	1.28	± 0.05 ^{b}	0.68	± 0.07 ^{c}
20-40	1.29	± 0.01 ^{a}	0.356	± 0.014 ^{d}	0.082	± 0.001 ^{bc}	0.459	± 0.002 ^{c}	2.01	± 0.03 ^{d}	1.8	± 0.05 ^{d}	1.26	± 0.03 ^{b}	0.45	± 0.03 ^{ab}
40-60	1.32	± 0.01 ^{ab}	0.326	± 0.013 ^{cd}	0.077	± 0.003 ^{ab}	0.447	± 0.006 ^{abc}	1.95	± 0.04 ^{cd}	1.7	± 0.06 ^{cd}	1.27	± 0.04 ^{b}	0.54	± 0.05 ^{ab}
60-80	1.35	± 0.02 ^{bc}	0.303	± 0.012 ^{bc}	0.084	± 0.001 ^{bc}	0.454	± 0.003 ^{bc}	1.87	± 0.04 ^{bc}	1.5	± 0.07 ^{b}	1.19	± 0.02 ^{ab}	0.58	± 0.03 ^{bc}
80-100	1.41	± 0.01 ^{d}	0.258	± 0.005 ^{a}	0.084	± 0.002 ^{c}	0.445	± 0.004 ^{ab}	1.75	± 0.01 ^{a}	1.3	± 0.02 ^{a}	1.17	± 0.02 ^{a}	0.7	± 0.02 ^{c}
p-value	<0.0001		<0.0001		0.0212		0.0333		0.0001		<0.0001		0.01		0.0018	

ϱb: bulk density, θ_f: field capacity, θ_r: residual volumetric water content, θ_s: saturated volumetric water content, α and n: appropriate parameters of water curve characteristics in the soil, K_s: saturated hydraulic conductivity, K_0: initial hydraulic conductivity. [a,b,c]: Values in each column with different letters indicate significant differences in soil depth (post hoc LSD Fisher, $p < 0.05$). The results include means ± SE ($n = 4$).

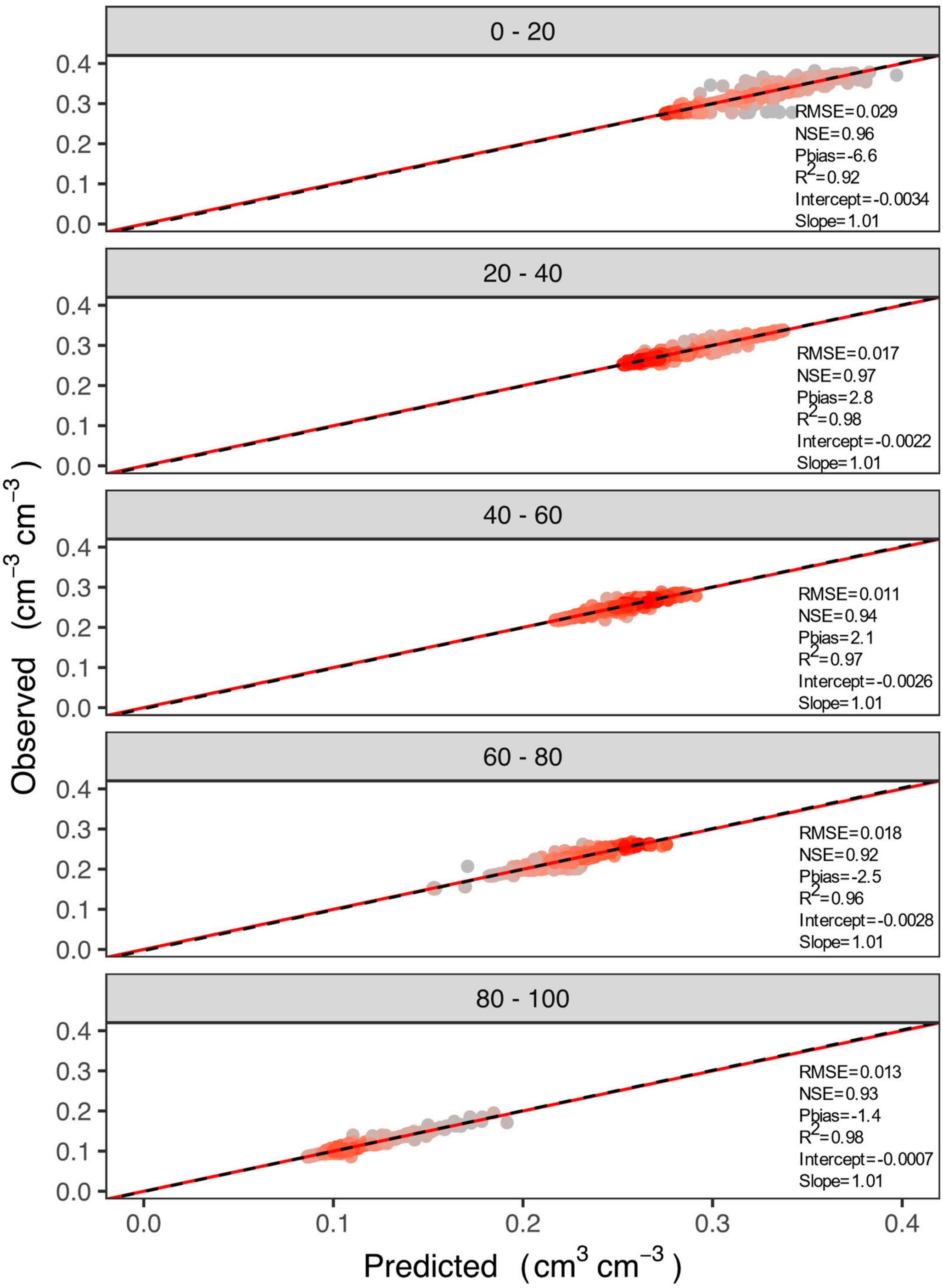

Figure 3. Linear regression between observed volumetric soil water content (y-axis) versus predicted values (x-axis) ($p<0.0001$ in all cases) is shown as dashed lines (the red line represents y=x) on the soil profile. The Root Mean Square Error (RMSE), Nash-Sutcliffe efficiency (NSE), Percent Bias (Pbias), and coefficient of determination (R^2) are given. The gradient from gray to red means from lower to higher density of points.

4. Discussion

4.1. Microclimatic conditions, water content and soil properties under agroforestry systems

The AFS have been shown to influence environmental variables, which affect the water status of cocoa farms, as well as the distribution of water in the soil profile [25,26]. Under AFS, trees used as shade canopy regulate the transmitted radiation affecting soil evaporation and leaf

Preprints (www.preprints.org) | NOT PEER-REVIEWED | Posted: 20 October 2023 doi:10.20944/preprints202310.1283.v1

transpiration[43,44] and consequently the vapor pressure deficit (VPD) and evapotranspiration (ET_0)[45,46]. These environmental drivers can lead to direct and indirect effects on plant and crop physiological functioning (stomatal conductance, gas exchange, sap flow velocity)[25,47,48], which in turn, depending on the water adjustment made by soil-plant-atmosphere, translates into a direct effect on soil water content availability[7,33,49].

Given the mechanisms and processes discussed above, our study showed that ET_0 dynamics depend mostly on soil water availability from rainfall events. Between each rainfall event, it was observed that water moved through the soil profile, and due to percolation, availability was reduced in the first centimeters of depth[50], significantly increasing percolation, which allowed a high water content to be observed in the soil profile during the entire monitoring[51]. This is due to the mechanism that relates the precipitation variability with the displacement of the location of water availability in the soil profile, which results in a disproportionate increase in the depth of water penetration with the amount of precipitation[52]. In addition, depending on the amount of water (mm) that reached the soil by precipitation, the soil presented a sensitivity in volumetric water content (θ) instantaneously, there being a short-term preferential flow during rainfall events that can generate infiltration through the soil profile[53].

On the other hand, there are soil characteristics that affect ET, which are related to bulk density (ϱb) and organic carbon content[54]. For example, ϱb increased proportionally to depth, however, probably due to the action of the root system ϱb was reduced between 20 and 40 cm depth[55,56]. Studies have described that the cocoa crop tends to present a greater concentration of roots in the first 60 cm of depth to capture a greater amount of water[57,58], a situation that modifies the ϱb. Likewise, small-scale determinations of soil texture and organic carbon content (CO%) showed different variations within the soil profile. For example, between 20 and 60 cm, a higher clay content (clay loam) was found, a condition that affected water mobility in the soil profile[13] as well as the amount of CO in the soil, which was 2% in the first 10 cm of depth, an amount that was reduced by half after 60 cm, conditions that have been described as causing the modification of water availability in the soil[59]. In addition to the above, the field capacity (θf) in the soil profile was inversely proportional to the ϱb, specifically in the zone with the highest concentration of roots[50,60–62] as well as a relationship was also found in this way between ϱb and θ_f with moisture content, as well as with clay and organic matter content that favored a higher soil saturated water content (θ_s)[63,64].

4.2. Hydrological properties of the soil

Soil physics (texture, bulk density) influenced the hydrological properties of the soil as well as water availability related to infiltration, percolation, surface runoff, inter (or soil) flow and groundwater flow[59,65] in the soil profile. For example, our study found that saturated water content (θ_s) presented significant differences at the soil depth level, with higher saturation at the 20-40 cm depth corresponding to the soil layer with higher root density[66]. In addition to the above, a higher θ_s was related to clay texture, which has a maximum water holding capacity and a minimum water release property[67,68]; furthermore, a significant effect of θ_s on K_s and n values was observed where small changes in θ_s promoted variations of n and K_s throughout the soil profile[69].

On the other hand, soil water retention is mainly related to changes in bulk density and its magnitude depends on soil texture[70,71]. Likewise, the soil water retention function is subject to the hysteresis phenomenon, which manifests itself as a difference between the soil wetting and drying equilibrium curves (hysteresis cycle)[72]. Based on the above, in our study, we presume that a hysteresis phenomenon is present in the soil profile due to changes in water availability in the soil profile (θ) due to multiple rainfall events; added to this, variations in soil texture (sandy clay loam and clay loam), generated a bottle effect due to the lack of uniformity in the shape and sizes of both individual pores and interconnected pore networks[73,74]. As a consequence, the parameter α, which is more related to soil structure, is more affected by the different wetting processes[75]; in addition, these conditions caused the residual water content (θ_r) to present variations in the soil profile due to higher suction (i.e., loam and clay loam soils with higher α values), as we observed in the depth of 20-40 cm[68,76], which causes almost all soil pores to remain filled with water at high tensions[72].

Preprints (www.preprints.org) | NOT PEER-REVIEWED | Posted: 20 October 2023 doi:10.20944/preprints202310.1283.v1

For the case of parameter n, it presented greater stability as it was associated with texture than with soil structure[77], presenting the lowest values in the soil with the sandiest fraction (at depths 0-20 and 60 -100 cm) and higher values in the most clayey texture (depths 20-60 cm)[68,78]. It should also be noted that the low variability of n values may result in a considerably different shape of the soil water retention curve[77].

The dynamics of soil structure and its associated factors (e.g., root biomass, root system activity, soil fauna, and organic matter input) decrease with soil depth[79,80]. This trend causes saturated hydraulic conductivity (K_s) to decrease with increasing soil depth[81]. Our study found that these factors can influence K_s in the first 20 cm depth. Moreover, the results obtained were in agreement with da Silva et al.[82] and Marques et al.[83], who, when analyzing K_s with different vegetation types in the lower Amazon, found higher values of this property at the surface, alluding that K_s is more sensitive to changes in soil properties. Also, our results indicated that a high contribution of organic matter (by the accompanying trees and cocoa) in the surface layer improves the structure and influences the hydraulic and translocation properties of clay, forming very hard layers in some depths. This effect caused that when observing the behavior of K_s by depth, a relationship between K_s decrease with depths with higher clay content was found [84,85]. In addition, we found a highly significant relationship between decreases in K_s and θ_f with increases in K_0 and ϱb in the soil profile[86], as a positive correlation between Ks and θs values, which may be associated with the presence of larger pores[77].

4.3. Hydrus-1D Calibration and Validation Model

Under field conditions, soil properties exhibit variations in vertical and horizontal directions[66]. Also, soil hydraulic properties that control soil water dynamics and redistribution vary from one point to another[66]. Thus, in this study, the van Genuchten model was selected to determine soil hydraulic properties and water retention variables (θ_f, θ_s, α, n, K_s). By inverse modeling, the observed and simulated soil water content was adjusted by the Rosetta pedotransfer function[20,87]. In this sense, the results between observed and simulated data presented very similar variation trends, with values in water content (θ) estimated close to the observed data [82]. The HYDRUS-1D model was able to simulate the θ at the different depths accurately, the dynamics consistently reflect rainfall events and the data indicate that the observed soil water content is well represented by the modeling results, with R^2 values equal to 0.96 and 0.99[88]. However, some discrepancies were observed between the measured and simulated θ, specifically on day 81 of 2015 (March 22), indicating that the model could not effectively capture the observed data, particularly for high values. This same observation was obtained by Raki et al.[89], Silva et al.[82] and Greccoa et al.[90] where they concluded an underestimation where the model did not respond to small precipitation events that occurred in short periods, overestimating the θ values measured in the field relating them to the high infiltration rate considered by the model, as well as overestimating evapotranspiration rates, which can reduce soil water content. In addition, Rezaei et al.[91], similar to us, associated the small variations between simulated and observed values to the soil hysteresis phenomenon, as discussed above.

The simulated and observed values of soil water content presented R^2 that ranged from 0.96 for the 20 cm depth to 0.99 for the other depths (40, 60, 80, 100) and the RMSE values ranged in minimal values (0.00002 to 0.00003). Being the depth of 60 the one that presented the lowest RMSE (0.0002), where a higher and almost constant θ was observed[66]. In this sense, the simulated values of soil hydraulic parameters such as it θ were close to the measured ones. The above shows the capability of the HYDRUS-1D software to simulate field conditions, even under agroforestry systems [92]. Moreover, this method and the goodness of fit produced the smallest variations, thus obtaining a great prediction[93,94]. Considering the above results and the entire time series used, both simulation and validation, for use in the HYDRUS-1D model describe well the soil conditions under the cocoa-woody agroforestry system. Also, we believe that simulation based on field data can reproduce the water movement and change process more accurately[68]. Also, the impact of hysteresis on the soil

 doi:10.20944/preprints202310.1283.v1

water content process needs to be further considered to improve the simulation accuracy and model results[95].

5. Conclusions

When modeling the volumetric soil water content (θ, cm^3 cm^{-3}) under agroforestry systems (SAF) with cocoa, a small bias was found as a high level of coherence between the observed values, based on the goodness of model fit measured by the Root Mean Square Error (RMSE), Nash-Sutcliffe efficiency (NSE), Percent Bias (Pbias), and coefficient of determination (R^2). During the monitoring period, it was found that cocoa cultivation under agroforestry systems presented a negative climatic water balance, a water status that requires considerable attention since evapotranspiration (ET_0) conditions greater than 5 mm d^{-1} were present in conditions where the radiation was greater than 1,041 μmol m^{-2} s^{-1}, with relative humidity levels in the atmosphere of 45% and higher ambient temperatures of 32.2 ºC that generated a vapor pressure deficit of 1.6 kPa, which can be worrying in current conditions of climatic variation with a tendency to temperature increases.

Author Contributions: Conceptualization, F.B., J.C.S., and F.A.O-M.; methodology, F.B., J.C.S., and F.A.O-M.; software, J.C.S., validation, F.B., J.C.S., and F.A.O-M.; formal analysis, F.B., J.C.S., and F.A.O-M.; investigation, F.B., and J.C.S.; resources, F.B., J.C.S., and F.A.O-M.; data curation, F.B., J.C.S., and F.A.O-M.; writing—original draft preparation, F.B., J.C.S., and F.A.O-M.; writing—review and editing, F.B., J.C.S., and F.A.O-M.; visualization, F.B., J.C.S., and F.A.O-M.; supervision, J.C.S.; project administration, J.C.S.; funding acquisition, J.C.S., All authors have read and agreed to the published version of the manuscript.

Funding: This research received no external funding.

Institutional Review Board Statement: Not applicable.

Informed Consent Statement: Not applicable.

Data Availability Statement: Data are available from the authors upon request.

Acknowledgments: We appreciate the support of the University of the Amazon for all the collaboration provided in the implementation and development of the experiment to determine the water status of cocoa in the agroforestry systems with cocoa implemented in the Amazonian research center CIMAZ Macagual. To the doctoral program in Natural Sciences and Sustainable Development of the Faculty of Agricultural Sciences of the University of the Amazon.

Conflicts of Interest: The authors have declared that no competing interests exist.

References

1. Seki K, Ackerer P, Lehmann F. Sequential estimation of hydraulic parameters in layered soil using limited data. Geoderma. 2015 Jun 1;247–248:117–28.
2. Seneviratne SI, Corti T, Davin EL, Hirschi M, Jaeger EB, Lehner I, et al. Investigating soil moisture–climate interactions in a changing climate: A review. Earth-Science Rev. 2010 May 1;99(3–4):125–61.
3. Vereecken H, Huisman JA, Pachepsky Y, Montzka C, van der Kruk J, Bogena H, et al. On the spatio-temporal dynamics of soil moisture at the field scale. J Hydrol. 2014 Aug 4;516:76–96.
4. Vanderlinden K, Vereecken H, Hardelauf H, Herbst M, Martínez G, Cosh MH, et al. Temporal Stability of Soil Water Contents: A Review of Data and Analyses. Vadose Zo J. 2012 Nov 1;11(4):vzj2011.0178.
5. Wang T, Wedin DA, Franz TE, Hiller J. Effect of vegetation on the temporal stability of soil moisture in grass-stabilized semi-arid sand dunes. J Hydrol. 2015 Feb 1;521:447–59.
6. Bodner G, Scholl P, Loiskandl W, Kaul HP. Environmental and management influences on temporal variability of near saturated soil hydraulic properties. Geoderma. 2013 Aug 1;204–205:120–9.
7. Köhler M, Hanf A, Barus H, Hendrayanto, Hölscher D. Cacao trees under different shade tree shelter: effects on water use. Agrofor Syst [Internet]. 2014 Feb 24 [cited 2019 Jun 19];88(1):63–73. Available from: http://link.springer.com/10.1007/s10457-013-9656-3
8. Siles P, Harmand JM, Vaast P. Effects of Inga densiflora on the microclimate of coffee (Coffea arabica L.) and overall biomass under optimal growing conditions in Costa Rica. Agrofor Syst [Internet]. 2010 Jun 28 [cited 2021 Aug 16];78(3):269–86. Available from: https://link.springer.com/article/10.1007/s10457-009-9241-y
9. Siles P, Vaast P, Dreyer E, Harmand JM. Rainfall partitioning into throughfall, stemflow and interception loss in a coffee (Coffea arabica L.) monoculture compared to an agroforestry system with Inga densiflora. J Hydrol. 2010 Dec 6;395(1–2):39–48.

10. Van Kanten R, Vaast P. Transpiration of arabica coffee and associated shade tree species in sub-optimal, low-altitude conditions of Costa Rica. Agrofor Syst. 2006;67(2):187–202.
11. Fu T, Chen H, Zhang W, Nie Y, Wang K. Vertical distribution of soil saturated hydraulic conductivity and its influencing factors in a small karst catchment in Southwest China. Environ Monit Assess [Internet]. 2015 Feb 7 [cited 2021 Aug 16];187(3):1–13. Available from: https://link.springer.com/article/10.1007/s10661-015-4320-1
12. Ugarte Nano CC, Nicolardot B, Ubertosi M. Near-saturated hydraulic conductivity measured on a swelling silty clay loam for three integrated weed management based cropping systems. Soil Tillage Res. 2015 Jul 1;150:192–200.
13. Schwen A, Zimmermann M, Bodner G. Vertical variations of soil hydraulic properties within two soil profiles and its relevance for soil water simulations. J Hydrol. 2014 Aug 4;516:169–81.
14. Schwendenmann L, Veldkamp E, Moser G, Hölscher D, Köhler M, Clough Y, et al. Effects of an experimental drought on the functioning of a cacao agroforestry system, Sulawesi, Indonesia. Glob Chang Biol [Internet]. 2010 May 1 [cited 2020 Jul 5];16(5):1515–30. Available from: http://doi.wiley.com/10.1111/j.1365-2486.2009.02034.x
15. Cresswell H, Smiles D, Williams J. Soil structure, soil hydraulic properties and the soil water balance. Soil Res [Internet]. 1992 [cited 2021 Aug 16];30(3):265–83. Available from: https://www.publish.csiro.au/sr/sr9920265
16. Es HM van, Ogden CB, Hill RL, Schindelbeck RR, Tsegaye T. Integrated Assessment of Space, Time, and Management-Related Variability of Soil Hydraulic Properties. Soil Sci Soc Am J [Internet]. 1999 Nov 1 [cited 2021 Aug 16];63(6):1599–608. Available from: https://acsess.onlinelibrary.wiley.com/doi/full/10.2136/sssaj1999.6361599x
17. Roger-Estrade J, Richard G, Dexter AR, Boizard H, De Tourdonnet S, Bertrand M, et al. Integration of soil structure variations with time and space into models for crop management. A review. Agron Sustain Dev 2009 291 [Internet]. 2009 Jan [cited 2021 Aug 16];29(1):135–42. Available from: https://link.springer.com/article/10.1051/agro:2008052
18. Dane J., Topp G. Methods of Soil Analysis. Part 4. SSSA Book Ser. 5. SSSA, Madison, WI. In: Methods of Soil Analysis Part 4 Part 4 SSSA Book Ser 5 SSSA, Madison, WI. 2002.
19. Hopmans J., Šimunek J, Romano N, Durner W. Inverse methods. In: Dane J., Topp GC, editors. Methods of Soil Analysis Part 4 Part 4 SSSA Book Ser 5 SSSA, Madison, WI. 2002. p. 963–1008.
20. Schaap MG, Leij FJ, Van Genuchten MT. rosetta: a computer program for estimating soil hydraulic parameters with hierarchical pedotransfer functions. J Hydrol. 2001 Oct 1;251(3–4):163–76.
21. Martínez-Fernández J, González-Zamora A, Sánchez N, Gumuzzio A. A soil water based index as a suitable agricultural drought indicator. J Hydrol. 2015 Mar 1;522:265–73.
22. Shi J, Li S, Zuo Q, Ben-Gal A. An index for plant water deficit based on root-weighted soil water content. J Hydrol. 2015 Mar 1;522:285–94.
23. Purcell LC, Sinclair TR, McNew RW. Drought Avoidance Assessment for Summer Annual Crops Using Long-Term Weather Data. Agron J [Internet]. 2003 Nov 1 [cited 2021 Aug 16];95(6):1566–76. Available from: https://acsess.onlinelibrary.wiley.com/doi/full/10.2134/agronj2003.1566
24. Suárez JC, Ngo Bieng MA, Melgarejo LM, Di Rienzo JA, Casanoves F. First typology of cacao (Theobroma cacao L.) systems in Colombian Amazonia, based on tree species richness, canopy structure and light availability. Struik PC, editor. PLoS One [Internet]. 2018 Feb 5 [cited 2019 Jun 19];13(2):e0191003. Available from: https://dx.plos.org/10.1371/journal.pone.0191003
25. Suárez JC, Casanoves F, Bieng MAN, Melgarejo LM, Di Rienzo JA, Armas C. Prediction model for sap flow in cacao trees under different radiation intensities in the western Colombian Amazon. 2021 [cited 2021 Jun 10];11(1). Available from: http://www.nature.com/articles/s41598-021-89876-z
26. Ordoñez C, Suárez JC, Rangel, Saavedra Mora D. Los sistemas agroforestales y la incidencia sobre el estatus hídrico en árboles de cacao. Biotecnol en el Sect Agropecu y Agroindustrial [Internet]. 2020 [cited 2021 Feb 16];19(1):256–67. Available from: https://doi.org/10.18684/BSAA
27. Niinemets Ü, Botany TK-E and E, 2014 undefined. Photosynthetic responses to stress in Mediterranean evergreens: mechanisms and models. Elsevier [Internet]. 2018 [cited 2021 Aug 27]; Available from: https://www.sciencedirect.com/science/article/pii/S0098847213001925
28. Ramalho JC, Zlatev ZS, Leitão AE, Pais IP, Fortunato AS, Lidon FC. Moderate water stress causes different stomatal and non-stomatal changes in the photosynthetic functioning of Phaseolus vulgaris L. genotypes. Plant Biol. 2014 Jan;16(1):133–46.
29. Zuidema P, Leffelaar P, Gerritsma W, … LM-A, 2005 undefined. A physiological production model for cocoa (Theobroma cacao): model presentation, validation and application. Elsevier [Internet]. [cited 2021 Aug 27]; Available from: https://www.sciencedirect.com/science/article/pii/S0308521X04001325
30. Lima ALS, DaMatta F, Pinheiro HA, Totola MR, Loureiro ME. Photochemical responses and oxidative stress in two clones of Coffea canephora under water deficit conditions. Environ Exp Bot. 2002 May 1;47(3):239–47.

31. Carr MK V., Lockwood G. The water relations and irrigation requirements of cocoa (Theobroma cacao L.): A review. Exp Agric [Internet]. 2011 Oct 27 [cited 2019 Jun 19];47(4):653–76. Available from: https://www.cambridge.org/core/product/identifier/S0014479711000421/type/journal_article
32. Moser G, Leuschner C, Hertel D, Hölscher D, Köhler M, Leitner D, et al. Response of cocoa trees (Theobroma cacao) to a 13-month desiccation period in Sulawesi, Indonesia production of cocoa beans. Agroforest Syst [Internet]. 2010 [cited 2020 Dec 7];79:171–87. Available from: https://link.springer.com/content/pdf/10.1007/s10457-010-9303-1.pdf
33. Köhler M, Schwendenmann L, Hölscher D. Throughfall reduction in a cacao agroforest: tree water use and soil water budgeting. Agric For Meteorol [Internet]. 2010 Jul 15 [cited 2019 Jun 19];150(7–8):1079–89. Available from: https://www.sciencedirect.com/science/article/pii/S0168192310001012
34. Allen RG, Pereira LS, Raes D, Smith M. Evapotranspiración del cultivo. Guías para la Determ los requerimientos agua los Cultiv Estud FAO Riego y Dren. 2006;56.
35. Allen, R G; Pereira, L. S; Raes, D; Smith M. Crop evapotranspiration-Guidelines for computing crop water requirements-FAO Irrigation and drainage paper 56 [Internet]. Vol. 300, Fao, Rome. 1998 [cited 2021 Aug 27]. D05109 p. Available from: http://www.avwatermaster.org/filingdocs/195/70653/172618e_5xAGWAx8.pdf
36. Šimůnek J, Genuchten MT van, Šejna M. The HYDRUS-1D software package for simulating the one-dimensional movement of water,heat, and multiple solutes in variably-saturated media, Version 4.0. Department of Environmental Sciences, University of California Riverside, Riverside, California, USA. 2013.
37. van Genuchten MT. A Closed-form Equation for Predicting the Hydraulic Conductivity of Unsaturated Soils. Soil Sci Soc Am J [Internet]. 1980 Sep 1 [cited 2021 Aug 27];44(5):892–8. Available from: https://acsess.onlinelibrary.wiley.com/doi/full/10.2136/sssaj1980.03615995004400050002x
38. Cannavo P, Sansoulet J, Harmand JM, Siles P, Dreyer E, Vaast P. Agroforestry associating coffee and Inga densiflora results in complementarity for water uptake and decreases deep drainage in Costa Rica. Agric Ecosyst Environ. 2011 Jan 30;140(1–2):1–13.
39. Suárez JC, Melgarejo LM, Durán Bautista EH, Di Rienzo JA, Casanoves F. Non-destructive estimation of the leaf weight and leaf area in cacao (Theobroma cacao L.). Sci Hortic (Amsterdam). 2018;229.
40. Zambrano M. hydroGOF: Goodness-of-fit functions for comparison of simulated and observed hydrological time series. R Packag version 03-8. 2014;
41. R Development Core Team. R version 4.2.0 (2022-04-22) -- "Vigorous Calisthenics" Copyright (C) 2024 The R Foundation for Statistical Computing Platform: x86_64-apple-darwin17.0 (64-bit). 2023; Available from: https://www.r-project.org/
42. Di Rienzo J., Casanoves F, Balzarini M., Gonzalez L, Tablada M, Robledo CW. InfoStat versión 2021. Grupo InfoStat, FCA, Universidad Nacional de Córdoba, Argentina. URL http://www.infostat.com.ar. 2021.
43. Niether W, Armengot L, Andres C, Schneider M, Gerold G. Shade trees and tree pruning alter throughfall and microclimate in cocoa (Theobroma cacao L.) production systems. Ann For Sci [Internet]. 2018 Jun 1 [cited 2020 Jul 5];75(2):1–16. Available from: https://doi.org/10.1007/s13595-018-0723-9
44. Gerlach MD, Lozano-Baez SE, Castellini M, Guzman N, Gomez WA, Medina B. Low Cost and Easy to Implement Physical and Hydrological Soil Assessment of Shade-Grown Coffee in Santa Rosa, Guatemala. L 2023, Vol 12, Page 390 [Internet]. 2023 Jan 31 [cited 2023 Sep 4];12(2):390. Available from: https://www.mdpi.com/2073-445X/12/2/390/htm
45. Cocoletzi Vásquez E, Hipólito-Romero E, Ricaño-Rodríguez J, Ramos-Prado JM, Cocoletzi Vásquez E, Hipólito-Romero E, et al. Ecophysiological plasticity of Theobroma cacao L. clones in response to the structure and microclimate of agroforestry systems in Mexico. Bot Sci [Internet]. 2022 Oct 1 [cited 2023 Sep 4];100(4):960–76. Available from: http://www.scielo.org.mx/scielo.php?script=sci_arttext&pid=S2007-42982022000400960&lng=es&nrm=iso&tlng=en
46. Fraga Junior LS, Vellame LM, de Oliveira AS, da Silva Paz VP. Transpiration of young cocoa trees under soil water restriction. Sci Agric [Internet]. 2020 [cited 2020 Jul 5];78(2). Available from: https://www.scielo.br/scielo.php?pid=S0103-90162021000200503&script=sci_arttext
47. Suárez JC, Melgarejo LM, Casanoves F, Di Rienzo JA, DaMatta F, Armas C. Photosynthesis limitations in cacao leaves under different agroforestry systems in the Colombian Amazon. Lambreva MD, editor. 2018 Nov 1 [cited 2019 Jun 19];13(11):e0206149. Available from: http://dx.plos.org/10.1371/journal.pone.0206149
48. Suárez JC, Gelpud C, Noriega JE, Ortiz-Morea FA. How do different cocoa genotypes deal with increased radiation? An analysis of water relation, diffusive and biochemical components at the leaf level. Agronomy [Internet]. 2021 [cited 2021 Aug 27];11(7). Available from: https://www.mdpi.com/2073-4395/11/7/1422
49. Balasimha D, Apshara E, Jose C. Genotypic variations in chlorophyll fluorescence and stomatal conductance of cocoa in relation to drought tolerance Genetic resources management of cocoa View project Statistical investigation on plantation crops View project. J Plant Crop [Internet]. 2013 [cited 2019 Jun 19];41(1):40–5. Available from: https://www.researchgate.net/publication/293133790

Preprints (www.preprints.org) | NOT PEER-REVIEWED | Posted: 20 October 2023 doi:10.20944/preprints202310.1283.v1

50. Padovan MP, Cortez VJ, Navarrete LF, Navarrete ED, Deffner AC, Centeno LG, et al. Root distribution and water use in coffee shaded with Tabebuia rosea Bertol. and Simarouba glauca DC. compared to full sun coffee in sub-optimal environmental conditions. Agrofor Syst [Internet]. 2015 Oct 22 [cited 2023 Sep 17];89(5):857–68. Available from: https://link.springer.com/article/10.1007/s10457-015-9820-z
51. Sala OE, Gherardi LA, Peters DPC. Enhanced precipitation variability effects on water losses and ecosystem functioning: differential response of arid and mesic regions. Clim Change [Internet]. 2015 Jul 1 [cited 2023 Sep 17];131(2):213–27. Available from: https://link.springer.com/article/10.1007/s10584-015-1389-z
52. Sala OE, Lauenroth WK, Parton WJ. Long-term soil water dynamics in the shortgrass steppe. Ecology [Internet]. 1992 Aug 1 [cited 2023 Sep 17];73(4):1175–81. Available from: https://onlinelibrary.wiley.com/doi/full/10.2307/1940667
53. Kulasekera PB, Parkin GW, von Bertoldi P. Using Soil Water Content Sensors to Characterize Tillage Effects on Preferential Flow. Vadose Zo J. 2011 May 1;10(2):683–96.
54. Perrin AS, Fujisaki K, Petitjean C, Sarrazin M, Godet M, Garric B, et al. Conversion of forest to agriculture in Amazonia with the chop-and-mulch method: Does it improve the soil carbon stock? Agric Ecosyst Environ. 2014 Feb 1;184:101–14.
55. Müller MW, Gama-Rodrigues AC. Cacao agroforestry systems. In: Valle RR, editor. Science, technology and management of cacao tree CEPLAC/CEPEC, Ilhéus. 2012. p. 246–71.
56. Rico A A, Suárez S JC, Rico A A, Suárez S JC. Biomasa de raíces finas en arreglos agroforestales con cacao en la amazonia occidental colombiana. Rev Ciencias Agrícolas [Internet]. 2018 Jun 26 [cited 2023 Sep 17];35(1):26–35. Available from: http://www.scielo.org.co/scielo.php?script=sci_arttext&pid=S0120-01352018000100026&lng=en&nrm=iso&tlng=es
57. Nambiar EKS, Sands R. Effects of compaction and simulated root channels in the subsoil on root development, water uptake and growth of radiata pine. Tree Physiol [Internet]. 1992 Apr 1 [cited 2023 Sep 17];10(3):297–306. Available from: https://dx.doi.org/10.1093/treephys/10.3.297
58. Claus A, George E. Effect of stand age on fine-root biomass and biomass distribution in three European forest chronosequences. https://doi.org/101139/x05-079 [Internet]. 2011 Jul [cited 2023 Sep 17];35(7):1617–25. Available from: https://cdnsciencepub.com/doi/10.1139/x05-079
59. Zhou T, Han C, Qiao L, Ren C, Wen T, Zhao C. Seasonal dynamics of soil water content in the typical vegetation and its response to precipitation in a semi-arid area of Chinese Loess Plateau. J Arid Land [Internet]. 2021 Oct 1 [cited 2023 Sep 17];13(10):1015–25. Available from: https://link.springer.com/article/10.1007/s40333-021-0021-5
60. Jiménez F, Alfaro R, Jiménez F, Beer J. Available soil water in coffea arabica-Erythrina pueppigiana, C-arabica-Eucalyptus deglupta and C. arabica-monoculture plantation. In: International Symposium on Multi-Strata Agroforestry Systems with Perennial Crops, Turrialba (Costa Rica). 1999. p. 27.
61. Morales E, Beer J. Distribución de raíces finas de Coffea arabica y Eucalyptus deglupta en cafetales del Valle Central de Costa Rica. Agroforestería en las Américas [Internet]. 1998 [cited 2023 Sep 17];5(17–18). Available from: http://bco.catie.ac.cr:8087/portal-revistas/index.php/AGRO/article/view/825/980
62. Arévalo-Gardini E, Canto M, Alegre J, Loli O, Julca A, Baligar V. Changes in Soil Physical and Chemical Properties in Long Term Improved Natural and Traditional Agroforestry Management Systems of Cacao Genotypes in Peruvian Amazon. PLoS One [Internet]. 2015 Jul 16 [cited 2023 Sep 17];10(7):e0132147. Available from: https://journals.plos.org/plosone/article?id=10.1371/journal.pone.0132147
63. Persson M, Berndtsson R, Nasri S, Albergel J, Zante P, Yumegaki Y. Solute transport and water content measurements in clay soils using time domain reflectometry. https://doi.org/101080/02626660009492387 [Internet]. 2009 [cited 2023 Sep 17];45(6):833–47. Available from: https://www.tandfonline.com/doi/abs/10.1080/02626660009492387
64. Merdun H. Effects of different factors on water flow and solute transport investigated by time domain reflectometry in sandy clay loam field soil. Water Air Soil Pollut [Internet]. 2012 Sep 24 [cited 2023 Sep 17];223(8):4905–23. Available from: https://link.springer.com/article/10.1007/s11270-012-1246-x
65. Horel Á, Tóth E, Gelybó G, Kása I, Bakacsi Z, Farkas C. Effects of Land Use and Management on Soil Hydraulic Properties. Open Geosci [Internet]. 2015 Nov 24 [cited 2023 Sep 17];7(1):1442–54. Available from: https://www.degruyter.com/document/doi/10.1515/geo-2015-0053/html
66. Ndulue E, Mante AA, Ranjan RS. HYDRUS-1D Simulation of Soil Water Dynamics and Response of Different ETo Models to Crop Evapotranspiration (ETc) Under a Rainfed Condition in Southern Manitoba. 2021 Oct 5 [cited 2023 Sep 17]; Available from: https://www.researchsquare.com
67. Çakir R. Water holding properties and soil water types in fine textured Vertisol soils of Thrace region in Turkey. Polish J Soil Sci [Internet]. 2019 Nov 21 [cited 2023 Sep 17];52(2):247. Available from: https://journals.umcs.pl/pjss/article/view/8531
68. Zhang P, Chen G, Wu J, Wang C, Zheng S, Yu Y, et al. The Application and Improvement of Soil–Water Characteristic Curves through In Situ Monitoring Data in the Plains. Water 2022, Vol 14, Page 4012 [Internet]. 2022 Dec 8 [cited 2023 Sep 17];14(24):4012. Available from: https://www.mdpi.com/2073-4441/14/24/4012/htm

69. Moret-Fernández D, Latorre B, López M V., Pueyo Y, Tormo J, Nicolau JM. Hydraulic properties characterization of undisturbed soil cores from upward infiltration measurements. CATENA. 2021 Jan 1;196:104816.
70. Rawls WJ, Pachepsky YA, Ritchie JC, Sobecki TM, Bloodworth H. Effect of soil organic carbon on soil water retention. Geoderma. 2003 Sep 1;116(1–2):61–76.
71. Ojeda G, Perfect E, Alcañiz JM, Ortiz O. Fractal analysis of soil water hysteresis as influenced by sewage sludge application. Geoderma. 2006 Oct 1;134(3–4):386–401.
72. Moret-Fernández D, Latorre B. A novel double disc method to determine soil hydraulic properties from drainage experiments with tension gradients. J Hydrol. 2022 Dec 1;615:128625.
73. Bachmann J, Van Der Ploeg RR. A review on recent developments in soil water retention theory: Interfacial tension and temperature effects. In: Journal of Plant Nutrition and Soil Science [Internet]. 2002 [cited 2023 Sep 17]. p. 468–78. Available from: https://onlinelibrary.wiley.com/doi/abs/10.1002/1522-2624(200208)165:4%3C468::AID-JPLN468%3E3.0.CO;2-G
74. Maqsoud A, Bussière B, Mbonimpa M, Aubertin M. Hysteresis effects on the water retention curve: a comparison between laboratory results and predictive models. 2004;
75. Moret-Fernández D, Arrúe JL, Pérez V, López M V. A TDR-pressure cell design for measuring the soil-water retention curve. Soil Tillage Res. 2008 Jul 1;100(1–2):114–9.
76. Tao G, Li J, Zhuang X, Xiao H, Cui X, Xu W. Determination of the residual water content of SWCC based on the soil moisture evaporation properties and micro pore characteristics. Yantu Lixue/Rock Soil Mech. 2018;39:1256–1262.
77. Jirků V, Kodešová R, Nikodem A, Mühlhanselová M, Žigová A. Temporal variability of structure and hydraulic properties of topsoil of three soil types. Geoderma. 2013 Aug 1;204–205:43–58.
78. Carsel RF, Parrish RS. Developing joint probability distributions of soil water retention characteristics. Water Resour Res [Internet]. 1988 May 1 [cited 2023 Sep 17];24(5):755–69. Available from: https://onlinelibrary.wiley.com/doi/full/10.1029/WR024i005p00755
79. Chen C, Liu W, Jiang X, Wu J. Effects of rubber-based agroforestry systems on soil aggregation and associated soil organic carbon: Implications for land use. Geoderma [Internet]. 2017 Aug 1 [cited 2019 Jul 27];299:13–24. Available from: https://www.sciencedirect.com/science/article/pii/S0016706117300769
80. Jiang XJ, Liu W, Chen C, Liu J, Yuan ZQ, Jin B, et al. Effects of three morphometric features of roots on soil water flow behavior in three sites in China. Geoderma. 2018 Jun 15;320:161–71.
81. Jiang XJ, Chen C, Zhu X, Zakari S, Singh AK, Zhang W, et al. Use of dye infiltration experiments and HYDRUS-3D to interpret preferential flow in soil in a rubber-based agroforestry systems in Xishuangbanna, China. CATENA. 2019 Jul 1;178:120–31.
82. Da Silva GS, Da Silva JS, De Carvalho Pereira FA, Santana RA, Firmo RS, Sobrinho OPL. Spatial variability of the saturated hydraulic conductivity of soil in cocoa farming in RecÔncavo Baiano. Rev Caatinga [Internet]. 2019 Jul 1 [cited 2023 Sep 17];32(3):786–94. Available from: https://www.scielo.br/j/rcaat/a/SLpDsG8m56PSm9ZcqFjxkZK/?lang=en
83. Monroe PHM, Gama-Rodrigues EF, Gama-Rodrigues AC, Marques JRB. Soil carbon stocks and origin under different cacao agroforestry systems in Southern Bahia, Brazil. Agric Ecosyst Environ [Internet]. 2016 Apr 1 [cited 2019 Jul 27];221:99–108. Available from: https://www.sciencedirect.com/science/article/pii/S0167880916300342
84. Mainuri ZG, Owino JO. Effects of land use and management on aggregate stability and hydraulic conductivity of soils within River Njoro Watershed in Kenya. Int Soil Water Conserv Res. 2013 Sep 1;1(2):80–7.
85. Hidayat Y, Purwakusuma W, Wahjunie ED, Baskoro DPT, Rachman LM, Yusuf SM, et al. Characteristics of Soil Hydraulic Conductivity in Natural Forest, Agricultural Land, and Green Open Space Area. J Pengelolaan Sumberd Alam dan Lingkung (Journal Nat Resour Environ Manag [Internet]. 2022 Jul 5 [cited 2023 Sep 17];12(2):352–62. Available from: https://journal.ipb.ac.id/index.php/jpsl/article/view/40527
86. Fasinmirin JT. Saturated Hydraulic Conductivity (K θs) of a Sub-Tropical Ultisol under different Tillage Systems Capacity Lecture Theatre Hall, Ilorin, Kwara State-Nigeria View project ASSESSMENT AND FORECASTING OF THE IMPACT OF CLIMATE CHANGE ON AGRICULTURAL AND HYDROLOGICAL DROUGHT IN NIGERIA View project. 2015 [cited 2023 Sep 17];3(4):1000. Available from: https://www.researchgate.net/publication/317014864
87. Okamoto K, Sakai K, Nakamura S, Cho H, Nakandakari T, Ootani S. Optimal Choice of Soil Hydraulic Parameters for Simulating the Unsaturated Flow: A Case Study on the Island of Miyakojima, Japan. Water 2015, Vol 7, Pages 5676-5688 [Internet]. 2015 Oct 20 [cited 2023 Sep 17];7(10):5676–88. Available from: https://www.mdpi.com/2073-4441/7/10/5676/htm
88. Lopes Da Silva JR, Antônio De Assunção Montenegro A, Luiz A, Monteiro N, De Paula V, Junior S. Modelagem da dinâmica de umidade do solo em diferentes condições de cobertura no semiárido pernambucano. Rev Bras Ciências Agrárias [Internet]. 2015 Jun 30 [cited 2023 Sep 17];10(2):293–303. Available from: http://www.agraria.pro.br/ojs32/index.php/RBCA/article/view/v10i2a4219

89. Er-Raki S, Ezzahar J, Merlin O, Amazirh A, Hssaine BA, Kharrou MH, et al. Performance of the HYDRUS-1D model for water balance components assessment of irrigated winter wheat under different water managements in semi-arid region of Morocco. Agric Water Manag. 2021 Feb 1;244:106546.
90. Grecco KL, Miranda JH d., Silveira LK, van Genuchten MT. HYDRUS-2D simulations of water and potassium movement in drip irrigated tropical soil container cultivated with sugarcane. Agric Water Manag. 2019 Jul 20;221:334–47.
91. Rezaei M, Seuntjens P, Shahidi R, Joris I, Boënne W, Al-Barri B, et al. The relevance of in-situ and laboratory characterization of sandy soil hydraulic properties for soil water simulations. J Hydrol. 2016 Mar 1;534:251–65.
92. Mohammed E, Abid-Alziz AL-Qassab S, Salih AL-Wazan FA, Mohammed E, Abid-Alziz AL-Qassab S, Salih AL-Wazan FA. Using Inverse Modeling by HYDRUS-1D to Predict Some Soil Hydraulic Parameters from Soil Water Evaporation. Colomb For [Internet]. 2022 Jan 1 [cited 2023 Sep 17];25(1):21–35. Available from: http://www.scielo.org.co/scielo.php?script=sci_arttext&pid=S0120-07392022000100021&lng=en&nrm=iso&tlng=en
93. Samani JMV, Fathi P. Estimation of unsaturated soil hydrodynamic parameters using inverse problem technique. J Agric Sci Technol [Internet]. 2009 [cited 2023 Sep 17];11(2):199–210. Available from: https://www.sid.ir/EN/VEWSSID/J_pdf/84820090205.pdf
94. Oliver YM, Smettem KRJ, Oliver YM, Smettem KRJ. Predicting water balance in a sandy soil: model sensitivity to the variability of measured saturated and near saturated hydraulic properties. Soil Res [Internet]. 2005 Feb 17 [cited 2023 Sep 17];43(1):87–96. Available from: https://www.publish.csiro.au/sr/SR03146
95. Brocca L, Ciabatta L, Massari C, Camici S, Tarpanelli A. Soil Moisture for Hydrological Applications: Open Questions and New Opportunities. Water 2017, Vol 9, Page 140 [Internet]. 2017 Feb 20 [cited 2023 Sep 17];9(2):140. Available from: https://www.mdpi.com/2073-4441/9/2/140/htm